An Integrated Approach Towards Process Planning for 5-axis Milling of Sculptured Surfaces Based on Cutter Accessibility Map

L. L. Li[1] and Y. F. Zhang[1]

[1]National University of Singapore, mpezyf@nus.edu.sg

ABSTRACT

In 5-axis milling (finish cut) of sculptured surfaces, the cutter's accessibility to the part surface is an important issue for subsequent process planning tasks. In this paper, a unique algorithm is presented to evaluate the accessibility of a cylindrical fillet-ended cutter to a point on the part surface by considering machine axis limit, avoidance of local-gouging, rear-gouging, and global-collision. By applying this algorithm to the sampled points of a given part surface, the accessibility map (A-map) of the cutter to any point on the part surface can be obtained. More significantly, the A-maps can be subsequently employed for optimal cutter selection, optimal cutting direction selection, and optimal tool-path generation. It is expected that by employing this concept, the process planning tasks for 5-axis milling of sculptured surfaces can be carried out in an integrated and efficient manner.

Keywords: cutter accessibility; cutter selection; cutting direction selection; tool path generation.

1. INTRODUCTION

Five-axis milling provides a powerful alternative for machining sculptured surfaces with complicated shapes. Compared to 3-axis machining, the 5-axis mode offers numerous advantages such as great reduction of set-up process, high machining efficiency and accuracy [12]. Take the effective cutting profile for example. In 5-axis milling, the cutter posture could be adjusted such that the cutting profile closely matches the part surface. However, the flexibility of changing cutter posture dynamically also introduces difficulty and complication into the tasks in process planning, since the search space of cutter posture is greatly expanded by the fact that the cutter can have an 'infinite' number of orientation postures at every point.

The process planning tasks for 5-axis milling (finish cut) include cutter selection and tool-path generation. The former determines the best cutter from the available ones that can traverse the entire surface without interference (local-gouging, rear-gouging, and global-collision). The latter selects a tool-path pattern, generates the cutter-contact (CC) points that satisfy the accuracy requirement, and determines the cutter's posture (orientation) at every CC point without causing any interference.

Currently, there is no commercially available Computer-aided Manufacturing (CAM) software package that provides comprehensive automatic process planning functions for 5-axis milling. On the other hand, there has been much research work to achieving automated process planning in this domain. The research issues addressed in reported literature include cutter selection [3], [5], tool-path pattern selection [2], [4], and interference-free tool-path generation [1], [6], [8-11], [13] to name a few. Generally speaking, of the reported work mainly focuses on tool-path generation by considering interference avoidance, scallop-height control, and cutting efficiency, in which the geometric issues have been well studied. However, it is also noticed that cutter selection and tool-path generation are treated as separate tasks, i.e., a cutter and cutter feeding direction is pre-determined before tool-path generation. Even among the limited reported work in cutter selection, a cutter is selected during tool-path generation in a trial-and-error manner. In fact, cutter selection should be addressed before tool-path pattern selection (including feeding direction) and tool-path generation. The issue to be addressed is to make sure that the cutter has an interference-free posture at every sampled point on the surface. The checking procedure is therefore, to a certain extent, similar to that of tool-path generation. At the same time, since the density of the sampled points can be easily higher than that of CC points (used for subsequent tool-path generation), the checking results from cutter selection can also be used for tool-path

pattern selection and tool-path generation. In this way, the process planning problems can be solved in an integrated and efficient manner.

In this paper, we address the process planning problems in an integrated manner based on the concept of cutter accessibility. When a cutter is placed with its cutting edge in contact with a point on the part surface, the *cutter accessibility to this point* refers to the posture range (in terms of the rotational and tilting angles) along which the cutter has no interference with the surface. Here, interference refers machine axis limit, local- and rear-gouging and global-collision. We call this posture range an accessibility map (A-map). Based on this concept, we have developed a point-based algorithm through geometric analysis to obtain the cutter A-map without consideration of feeding direction [7]. By applying this algorithm to all the sampled points on a part surface, we can judge whether the cutter can traverse the whole surface without any interference. The optimal cutter can therefore be selected by finding the A-maps of all the available cutters for machining the surface. Subsequently, the cutter A-map on the sampled points can be used for selecting the optimal feeding direction for a selected tool-path pattern. Furthermore, since the density of the sample points is generally much higher than that of the CC points, the cutter A-map at each CC points can be estimated through interpolation means and the final posture at each CC point can be determined based on various machining strategies. In this way, the process planning tasks can be conducted in an integrated and efficient manner.

The algorithm for obtaining the cutter A-map is briefly introduced in Section 2. Section 3 presents the applications of cutter A-map in the process planning for a 5-axis sculptured surface milling, including cutter selection, determination of iso-planar path direction, and tool-path generation. In Section 4, an example is given to show the effectiveness of the developed algorithms. Finally, conclusion remarks are given in Section 5. The cutter considered in this paper is a cylindrical cutter with a fillet-end, which also covers the flat-end cutter and the ball-end cutter.

2. CUTTER ACCESSIBILITY MAP

In this section, a point-based algorithm is briefly introduced to evaluate the A-map of a cutter to a point on a part surface. For more details, readers can refer to Li and Zhang [7]. There are four interference attributes to a cutter's accessibility to a point on the surface: the machine axis limit, avoidance of local-gouging, rear-gouging, and global-collision. The accessible range in terms of each interference attribute is first identified. The A-map of the cutter at a point is then established as the intersection of the four accessible ranges. Shown in Fig. 1 are the geometries of the cutter at a point ($\mathbf{P}_c$) on the part surface. A fillet-end cutter is described by its major radius (R), minor radius (r_f), and length (L). There are three coordinate frames used in the accessibility analysis. Machine frame ($\boldsymbol{X}$, $\boldsymbol{Y}$, $\boldsymbol{Z}$) is the universal coordinate system related to the machine configuration. Local frame ($\boldsymbol{X}_L$, $\boldsymbol{Y}_L$, $\boldsymbol{Z}_L$) is defined according to the surface geometry at $\mathbf{P}_c$. It originates at $\mathbf{P}_c$ with $\boldsymbol{Z}_L$-axis along the normal vector, $\boldsymbol{X}_L$-axis along the surface maximum principal direction, and $\boldsymbol{Y}_L$-axis along the surface minimum principal direction. A cutter's orientation is defined by an angle pair (λ, θ) meaning that the cutter's axis inclines counter-clockwise by λ about $\boldsymbol{Y}_L$-axis and rotates by θ about $\boldsymbol{Z}_L$–axis, where $0° \le \lambda \le 90°$ and $0° \le \theta \le 360°$. Tool frame ($\boldsymbol{X}_T$, $\boldsymbol{Y}_T$, $\boldsymbol{Z}_T$) is defined with its origin at the cutter bottom centre while $\boldsymbol{Z}_T$-axis along the cutter axis direction. The intersection line between the bottom plane and the plane defined by $\boldsymbol{Z}_T$-axis and $\mathbf{P}_c$ defines the $\boldsymbol{X}_T$-axis that points towards $\mathbf{P}_c$. The $\boldsymbol{Y}_T$-axis is defined by $\boldsymbol{Y}_T = \boldsymbol{Z}_T \times \boldsymbol{X}_T$. θ is 0 when $\boldsymbol{X}_L$-axis and $\boldsymbol{X}_T$-axis are co-planar, and $\lambda = 0$ when the $\boldsymbol{Z}_L$-axis and $\boldsymbol{Z}_T$-axis are parallel. The accessibility map is represented in terms of (λ, θ) in the local frame.

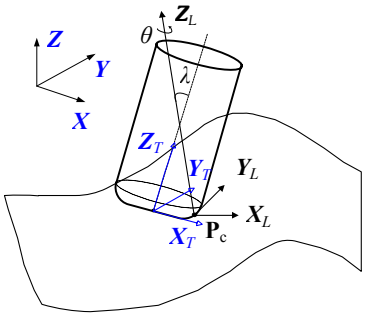

Fig. 1. The geometries of a cutter at a point $\mathbf{P}_c$ on the part surface.

2.1 A-map Based on Machine Axis Limits

A 5-axis machine tool typically has two revolute joints, each having a permissible range of angular positions. The limits are given in machine frame as a bounded region. The A-map based on the machine axis limits can be obtained through transformation between global frame and local frame. The boundary of the machine axis limits is firstly uniformly sampled into a set of points, each corresponding to an angle pair. These boundary points are then transformed from the machine frame to the local frame. By linking the corresponding boundary points in the local frame, we obtain a bounded region of (λ, θ), which is the A-map in respect to machine axis limits. One can read this map as, for every θ_i ($\theta_{min} \leq \theta \leq \theta_{max}$), there exits a range of λ, [$\lambda_{i\text{-}min}$, $\lambda_{i\text{-}max}$]. An example is shown in Fig. 2 to illustrate this procedure. Fig. 2a shows a point $\mathbf{P}_c$ on a sculptured surface. Fig. 2b shows the machine axis limits in the machine frame, and Fig. 2c shows the corresponding A-map in the tool frame at $\mathbf{P}_c$.

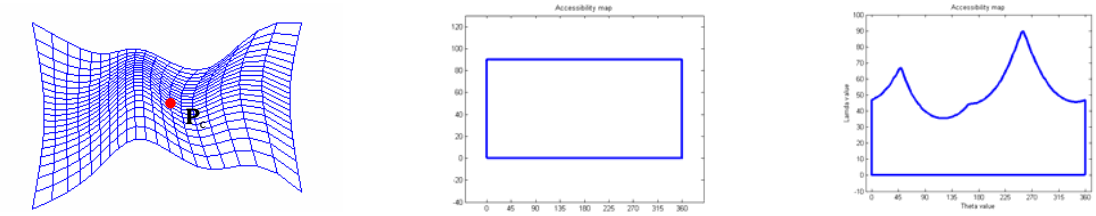

(a) A point $\mathbf{P}_c$ on a sculpture surface (b) Machine axis limits in machine frame (c) A-map in local frame

Fig. 2. Accessibility map based on machine axis limits.

2.2 A-map Based on Local-gouging Avoidance

Local-gouging occurs when the curvatures of the cutter's local surface are less than those of the part surface at the CC point such that the cutter cuts excess material. Therefore, given a posture (λ, θ) of the cutter, the normal curvatures of the cutter and the part surface at the CC point in every possible direction need to be compared to ensure the avoidance of local-gouging. At a point $\mathbf{P}_c$, the normal curvatures refer to the curvature of the surface curves (for both cutter surface and part surface) passing through the point and on a normal plane, as shown in Fig. 3a. To avoid local-gouging, given a θ, the range of λ must ensure that the normal curvature of the cutter surface curve must be no less than the normal curvature of the part surface curve. Mathematically, it has been proven that the conditions for local-gouging avoidance are given as follows [7]:

$$\sin\lambda > \frac{(R\text{-}r_f)(r_f\kappa_{max} - \cos^2\theta)}{r_f(1 - r_f\kappa_{max})} \tag{1}$$

$$\sin\lambda > \frac{(R\text{-}r_f)[\kappa_{max}(1 - r_f\kappa_{min}) - (\kappa_{max} - \kappa_{min})\cos^2\theta]}{(1 - r_f\kappa_{min})(1 - r_f\kappa_{max})} \tag{2}$$

Where R and r_f are the major and minor radii of the cutter respectively. κ_{max} and κ_{min} are the maximum and minimum principle normal curvatures of the surface at $\mathbf{P}_c$, respectively. To obtain the accessibility map of the cutter in respect of local-gouging, the range of θ in the A-map of machine axis limits, [θ_{min}, θ_{max}], is firstly sampled uniformly into a number of discrete angles. For every discrete θ_i, two minimum values of λ, $\lambda_{i\text{-}1}$ and $\lambda_{i\text{-}2}$, if there are any, can be obtained from Inequalities (1) and (2), respectively. At the same time, the accessible range for θ_i in terms of λ is [$\lambda_{i\text{-}min}$, $\lambda_{i\text{-}max}$], according to the A-map of machine axis limits. Therefore, the accessible range based on local-gouging avoidance becomes [$\lambda_{i\text{-}lg\text{-}min}$, $\lambda_{i\text{-}lg\text{-}max}$], where $\lambda_{i\text{-}lg\text{-}min}$ = max($\lambda_{i\text{-}min}$, $\lambda_{i\text{-}1}$, $\lambda_{i\text{-}2}$) and $\lambda_{i\text{-}lg\text{-}max}$ = $\lambda_{i\text{-}max}$. The A-map for local-gouging avoidance is simply the combination of all the [θ_i, ($\lambda_{i\text{-}lg\text{-}min}$, $\lambda_{i\text{-}lg\text{-}max}$)].

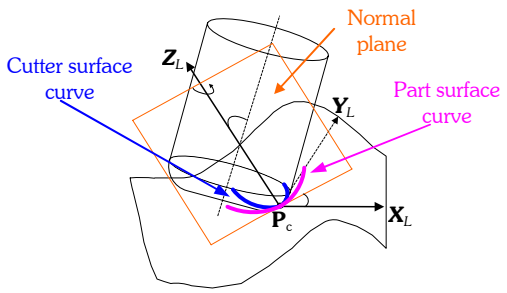

Fig. 3. Intersection curves between the normal plane and the part surface and cutter surface at the CC point.

2.3 A-map Based on Rear-gouging Avoidance

Rear-gouging occurs when the cutter bottom surface, including the circular plane and the filleted portion, protrudes into the part surface. To obtain the A-map based on rear-gouging avoidance, we follow a checking-and-correction approach. The range of θ in the A-map of machine axis limits, $[\theta_{min}, \theta_{max}]$, is firstly sampled uniformly into a number of discrete angles. For every discrete θ_i, we place the cutter along the posture of $(\theta_i, \lambda_{i\text{-min}})$ at $\mathbf{P}_c$ (see Fig. 4a). We then check whether the cutter causes rear-gouging with the part surface. To do that, the part surface is sampled into a number of discrete points and the checking is conducted between the cutter and all the sampled points (except $\mathbf{P}_c$). Take a sampled point P_j, for example, if P_j is inside the cutter's boundary and below the cylindrical portion, rear-gouging occurs. To correct this problem, the cutter is inclined clockwise by an increment of $\Delta\lambda_j$ such that P_j falls onto the cutter bottom surface. The cutter accessible posture range of rear-gouging avoidance with respect to P_j is $[\lambda_{i\text{-min}}+\Delta\lambda_j, \lambda_{i\text{-max}}]$. If P_j does not cause rear-gouging, $\Delta\lambda_j = 0$. The accessible range of rear-gouging avoidance at θ_i, $[\lambda_{i\text{-}rg\text{-min}}, \lambda_{i\text{-}rg\text{-max}}]$ is simply the intersection of the $[\lambda_{i\text{-}lg}+\Delta\lambda_j, \lambda_{i\text{-max}}]$, where $j = 1, \ldots, n$, and n is the total number of sampled points. The A-map for rear-gouging avoidance is the combination of all the $[\theta_i, (\lambda_{i\text{-}rg\text{-min}}, \lambda_{i\text{-}rg\text{-max}})]$.

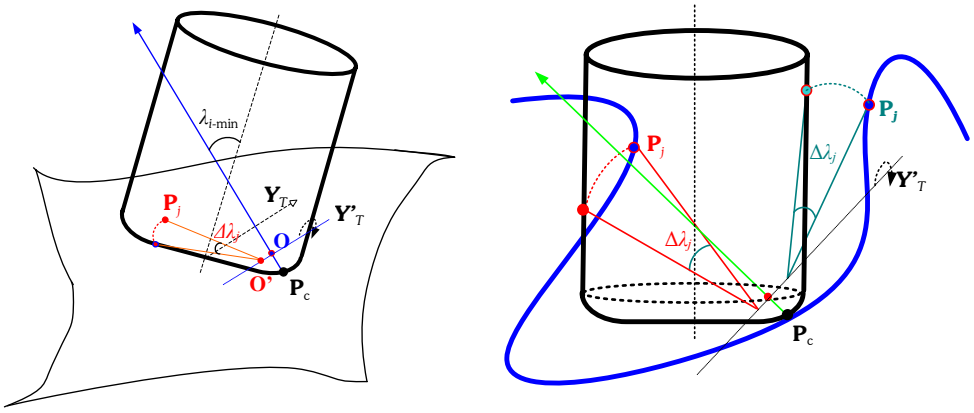

(a) Rear-gouging avoidance (b) Global-collision avoidance

Fig. 4. Obtaining A-maps based on rear-gouging and global-collision avoidance.

The following briefly shows the geometric analysis for the correction procedure. Referring to Fig. 4a, when θ is fixed and the cutter rotates to a different λ, the cutter will have different contact point on the filleted portion. Its pivot point **O** is along the normal vector of $\mathbf{P}_c$ with a distance r_f from $\mathbf{P}_c$. The rotation axis is $\mathbf{Y'}_T$ that is parallel to $\mathbf{Y}_T$-axis and passes through the pivot point **O**. Suppose $\mathbf{P}_j(x_j, y_j, z_j)$ causes rear-gouging, the intersection between the plane $y = y_j$ and the cutter bottom will produce a section curve and the plane intersects with $\mathbf{Y'}_T$ at **O'**. To correct the rear-gouging problem, we can simply rotate P_j clockwise about **O'** until it reaches the section curve. The angle increment $\Delta\lambda_j$ can be easily calculated in a 2D mode.

2.4 A-map Based on Global-collision Avoidance

Global collision occurs when the cutter shaft intersects with the part surface. In theory, given a posture, a point collides with the cutter if it falls "inside" the cylindrical portion of the cutter, in which the cutter length needs to be considered. Here, we consider that the point collides with the cutter if the distance between the point and the cutter axis is less than R, i.e., we assume the length of the cutter to be infinite. However, the constraints of the cutter's holder can also be considered in a similar manner if the geometry of the holder is given.

The method to obtain the A-map based on global collision avoidance also follows a checking-and-correction approach. The discrete values of θ used in rear-gouging analysis and the sampled points of the part surface are used here. For every discrete θ_i, we place the cutter along the posture of (θ_i, $\lambda_{i\text{-min}}$) at $\mathbf{P}_c$ (see Fig. 4b). We then check whether there exists any collision between the cutter and the sampled points (except $\mathbf{P}_c$). Take a sampled point $\mathbf{P}_j$, for example, if the distance between $\mathbf{P}_j$ and the cutter's axis is less than R, global collision occurs. In this case, $\mathbf{P}_j$ must be at the left of the cutter. To correct this problem, the cutter is inclined clockwise by an increment of $\Delta\lambda_j$ such that P_j falls onto the cutter cylindrical surface. The cutter accessible range of global-collision avoidance with respect to P_j is $[\lambda_{i\text{-min}}+\Delta\lambda_j, \lambda_{i\text{-max}}]$. If, however, $\mathbf{P}_j$ does not cause collision but is located in front of the cutter during forward inclination ($\mathbf{P}_j$ on the right), we need to find the $\Delta\lambda_j$ the cutter is inclined clockwise such that $\mathbf{P}_j$ touches the cutter cylindrical surface. In this case, the cutter accessible range of global-collision avoidance with respect to P_j becomes $[\lambda_{i\text{-min}}, \Delta\lambda_{i\text{-min}}+\Delta\lambda_j]$. Other than the above two scenarios, the cutter accessible range of global-collision avoidance with respect to P_j is $[\lambda_{i\text{-min}}, \lambda_{i\text{-max}}]$. The cutter accessible range of global-collision avoidance at θ_i, $[\lambda_{i\text{-}gc\text{-min}}, \lambda_{i\text{-}gc\text{-max}}]$, is simply the intersection of the cutter accessible ranges with respect to all the sampled points. The A-map for global-collision avoidance is the combination of all the $[\theta_i, (\lambda_{i\text{-}gc\text{-max}}, \lambda_{i\text{-}gc\text{-max}})]$. The geometric analysis for the correction procedure is similar to that of rear-gouging avoidance.

Up to now, the methods to obtain the A-maps based on the 4 attributes are briefly described. The A-map for the cutter at a point on the part surface is simply the intersection of its 4 individual A-maps. For the example shown in Fig. 2a, the other 3 A-maps based on the avoidance of local-gouging, rear-gouging, and global-collision are shown in Fig. 5a-c respectively. The intersection of these 4 A-maps is the hatched region shown in Fig. 5d, which is the A-map of the cutter at P_c. Note that the initial range of λ used for obtaining the A-maps of local-gouging, rear-gouging, and global is set as [0°, 90°], instead of the range from the A-map based on machine axis limits. This, however, does not affect the final A-map.

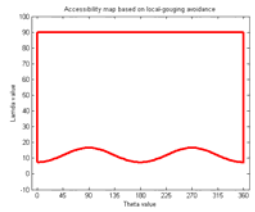

(a) A-map based on local-gouging avoidance

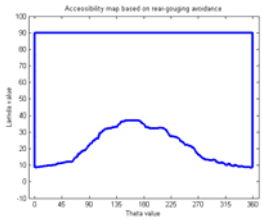

(b) A-map based on rear-gouging avoidance

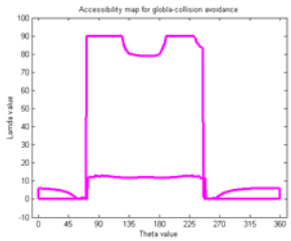

(c) A-map based on global-collision avoidance

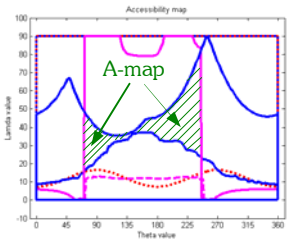

(d) The overall A-map at the point

Fig. 5. A Cutter's A-map at a point on the part surface.

3. APPLICATION OF A-MAP IN AUTOMATED PROCESS PLANMNING

The A-map represents the posture range for a cutter to access a point on the part surface without interference. Apart from interference concerns, the other two factors to be considered in process planning for 5-axis milling are accuracy and cutting efficiency, which are also closely related to cutter posture. Therefore, A-map is a very important cutter-vs.-part property for process planning. In this section, we show the application of A-map in three process planning tasks: cutter selection, cutting direction for iso-planar tool paths, and tool path generation.

3.1 Optimal cutter selection

Assuming that a single cutter is to be used for finish cut of a part surface, the cutter selection task is to find the best cutter from the available ones that can traverse the entire part surface without interference. This task can be considered as a two-phase decision-making process. The first phase involves the identification of those suitable cutters, from the available cutter set, that can finish the entire surface. The second involves the selection of the best cutter from the feasible ones according to a pre-defined optimization criterion.

Theoretically, we can find whether a cutter is accessible to the entire part surface by obtaining the A-maps of the cutter to every point on the surface. A practical approach is to discretise the part surface according to a sampling strategy such that the resulted sampled points closely reflect the characteristics of the part surface. We can then obtain the A-maps of the cutter at the sampled points. If none of these A-maps is empty, we say that the cutter is accessible to the part surface. Since the gaps between the neighboring sampled points have not been checked, the density of the sampled points is preferably high thus reducing errors.

As for the optimization phase, maximum cutting efficiency is chosen as the criterion. Since the tool-paths and cutting parameters are yet to be determined, it is not possible to give a close estimation just based on cutter dimension. In material removal process, intuition suggests that a larger cutter will potentially have higher cutting efficiency than a smaller cutter. For two cylindrical cutters (fillet-end), the cutter with larger R is considered better than the other. In case that the two cutters have the same R, the cutter with smaller r_f is considered better. Based on this rule of thumb, we firstly arrange the available cutters in a top-down list in which any cutter is better the one just underneath it in terms of cutting efficiency. Next, the following algorithm is used to find the largest feasible cutter:

Algorithm: Cutter selection for finish-cut

Input: (a) A part surface
(b) A set of fillet-end cutters $\{\boldsymbol{T}_i, i = 1, 2, \ldots, m\}$ sorted from large to small.
Output: *The largest cutter to can finish the part surface*

(1) Sample the part surface into a set of discrete point $\{\mathbf{P}_j, j = 1, 2, \ldots, n\}$; set $i = 1$.
(2) IF $i > m$, output "no available cutter can finish the entire surface". Stop
(3) Pick $\boldsymbol{T}_i$ from the cutter list, set $j = 1$.
(4) If $j \le n$, obtain the A-map of $\boldsymbol{T}_i$ at $\mathbf{P}_j$, denoted as A-map ($\boldsymbol{T}_i$, $\mathbf{P}_j$). Otherwise, output "the largest feasible cutter is $\boldsymbol{T}_i$".
(5) If A-map ($\boldsymbol{T}_i$, $\mathbf{P}_j$) is "NULL", set $i = i + 1$, go to (2). Otherwise, set $j = j + 1$, go to (4).

3.2 Optimal Cutting Direction Selection

Among the finish-cut tool-path patterns used for machining sculptured surfaces, iso-planar (Cartesian) path is a popular choice in which the paths are produced by intersecting the part surface with parallel planes along a certain direction. Over the years, iso-planar path has received extensive attention owing to its robustness in almost every scenario, for example, the machining of compound and composite surface [2]. In this section, we show the use of A-maps of a cutter in determining the optimal cutting direction of iso-planar path.

There are generally two optimization objectives in the process to select a cutting direction for the iso-planar paths. The first one is that the selected direction should produce high machining efficiency or short tool-path length overall. The second is to maintain a smooth change of cutter postures, which is particularly crucial in high speed machining. At this stage, to consider these two criteria simultaneously without having the actual tool-paths and the corresponding postures, we propose an evaluation factor at every sampled point on the part surface: the posture change rate (PCR).

Given a sampled point **P** and one of its neighboring sampled points, $\mathbf{P}_{next}$, the PCR along the direction of $\mathbf{PP}_{next}$ is the difference between the two corresponding postures then normalized by the distance between the two points, given by,

$$\mathrm{PCR} = \frac{2\,|\,sin\alpha\,|}{|\,\mathrm{P}-\mathrm{P}_{next}\,|} \tag{3}$$

Where α is the angle between the two postures. If we can obtain the PCRs of all the sampled points $\{\mathbf{P}_i, i = 1, 2, \ldots, n\}$ along any given cutting direction, the direction that possesses the minimum ($\sum_{i=1}^{n}\mathrm{PCR}_i\ /n$) can be chosen as the one with the smoothest tool-path.

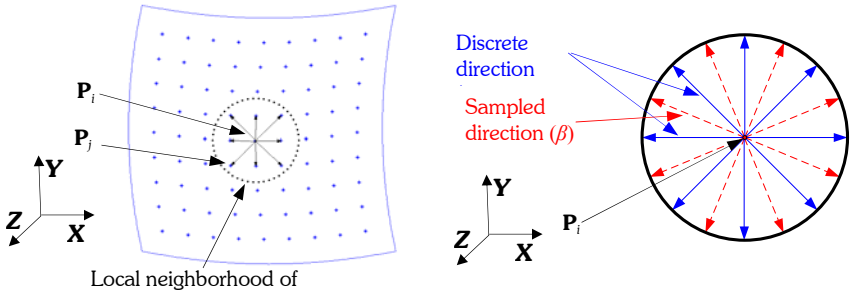

(a) Calculating $\mathrm{PCR}_{i,j}$ in the local neighborhood of $\mathbf{P}_i$

(b) Calculating PCR of $\mathbf{P}_i$ along the sampled directions

Fig. 6. Obtain the PCR of $\mathbf{P}_i$ along all the sampled cutting directions.

Now we show how to obtain the PCR at a sampled point, $\mathbf{P}_i$, along any cutting direction which is defined in the global frame, e.g., on the **X**-**Y** plane (see Fig. 6a). This is done in two steps. In the first step, we obtain the discrete PCRs of $\mathbf{P}_i$ based on the A-map at $\mathbf{P}_i$. As shown in Fig. 6a, a local neighborhood of $\mathbf{P}_i$ is firstly defined that contains m sampled points $\{\mathbf{P}_j, j = 1, 2, \ldots, m\}$. Vector $\mathbf{P}_i\mathbf{P}_j$ can be projected onto the X-Y plane, representing a discrete cutting direction $\beta_{i,j}$ ($0 \le \beta_{i,j} \le 2\pi$). At the same time, $\mathbf{P}_i\mathbf{P}_j$ corresponds to a rotational angle ω_i in the local frame at $\mathbf{P}_i$, representing the cutting direction. The selection of the cutter posture (θ_i, λ_i) at P_i along cutting direction ω_i is based on the following rule of thumb: θ_i should be preferable close to ω_i and λ_i should be as small as possible, thus producing the cutting stripe with the largest width [11]. From the A-map of $\mathbf{P}_i$, we can find θ_i, which is the closest to ω_i and take the minimum inclination angle λ_i corresponding to θ_i, to form the posture (θ_i, λ_i) at $\mathbf{P}_i$. Similarly, we can find the posture of the cutter at $\mathbf{P}_j$, (θ_j, λ_j). $\mathrm{PCR}_{i,j}$ can then be calculated using Eq. (3). In the second step, we obtain the PCR of $\mathbf{P}_i$ along any cutting direction β in the global frame, PCR_β, by making use of the discrete $\mathrm{PCR}_{i,j}$. Firstly, at P_i, we sample the range of $[0, 2\pi]$ uniformly into a number of discrete angle values βs, each corresponding to a cutting direction (see Fig. 6b). Take any direction along β, we find the two closest $\beta_{i,j}$ to β. PCR_β can then be obtained by applying linear interpolation of the two corresponding $\mathrm{PCR}_{i,j}$. Since the density of the sampled points is generally high, the linear interpolation should produce close results.

3.3 Tool-paths and CL Data Generation

In this section, we present an efficient algorithm to obtain the cutter location (CL) data for machining a part surface based on the A-maps of the sampled points and the determined cutting direction. The CL data refer to the CC points on the part surface and the corresponding cutter postures in (λ, θ) over the whole surface. Firstly, we show how to generate the CC points for a single tool-path based on pre-defined profile tolerance and determine the corresponding postures. Then, we show how to determine the step-over width between the current tool-path and the next one based on the scallop-height tolerance.

With the cutting direction fixed, the first tool-path can be generated by computing the intersection curve between the cutting plane and the part surface just off the edge of the surface. On the first path, we need to generate the CC points based on the profile tolerance. Since the first CC point on this path is already known, this generation process is effectively to determine the maximum step-forward length between the neighboring CC points. As shown in Fig. 7a, at CC point $\mathbf{P}_i$, the next point on the path, P_{i+1}, is determined such that the largest deviation d from the line segment

$\mathbf{P}_i\mathbf{P}_{i+1}$ to the part surface is very close to but less than the tolerance. Some reported solutions [11] can be employed for solving this problem.

For the newly generated CC point, we obtain its A-map by utilizing the known A-maps of the sampled points. This can be done by finding a small neighborhood of the CC point (e.g., 5 points) from the sampled points and taking the intersection of the 5 A-maps as the one for the CC point. With the A-maps of all the CC points on the current path, a certain machining strategy, such as minimum cutter posture change, can be applied to determine the cutter posture at each CC point.

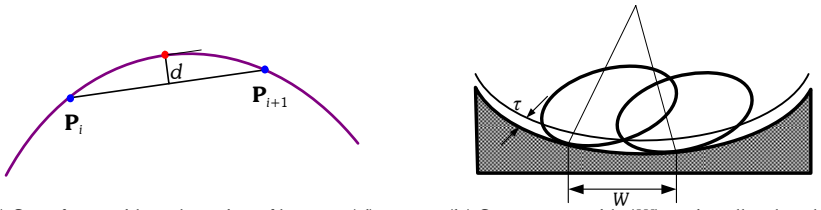

(a) Step-forward length and profile error (d) (b) Step-over width (W) and scallop height (τ)

Fig. 7. Step-forward length and step-over width.

Compared with step-forward length determination, step-over width is more difficult to determine since it is related not only to part surface geometry, but also the cutter postures at CC points on both paths. At each CC point on the current tool-path, the effective cutting shapes of the cutter bottom and the part surface need to be evaluated and the scallop height calculated, as shown in Fig. 7b. To obtain the largest allowable step-over width between the current and the next tool-paths, an adaptive approach is employed here. Firstly, the step-over widths (W_i) for all the CC points $\{P_i, i = 1, 2,\ldots,m\}$ on the current path are quickly estimated using the method introduced by Lin and Koren [9]. The smallest step-over width among $\{W_i, i = 1, 2,\ldots,m\}$ is set as the initial step-over width for the subsequent optimization process, which is described as follows:

(1) Compute the next tool-path using the step-over width.
(2) At every CC point of the current tool-path, find its corresponding CC point on the next tool-path and obtain its A-map (and a posture). Evaluate the cutting shapes at all the CC points of the current and next path. Calculate the scallop height τ_i at every CC point on the current path $\{P_i, i = 1, 2,\ldots,m\}$.
(3) If the largest τ_i is close to but less than the given scallop height tolerance, the optimal step-over width is found. Otherwise, Go to (4).
(4) If the scallop height at any CC point is larger than the given tolerance, reduce the step-over width by a certain proportion. Otherwise, increase step-over width by a certain proportion. Go back to (1).

There has been much research effort in computing the effective cutting shape and the scallop height, e.g., the method proposed by Lee [6], and the reported methods can be employed in this optimization procedure. This adaptive optimization idea may not be new. However, without the presence of the A-maps of the sampled points, it would be virtually impossible to implement it due to the heavy computation required to determine the cutter postures in the procedure.

4. AN EXAMPLE

In this section, we show the application of the aforementioned algorithms for the process planning to produce this part surface. Fig. 8a illustrates the geometry of a NURB surface patch, which consists of concave, convex and saddle regions. Tab. 1 shows a list of fillet-end cutters in a cutter library and all the cutters are sorted from large to small.

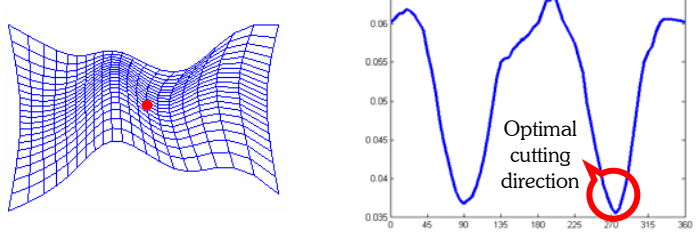

(a) A NURBs surface (b) The PCRs at the sampled cutting directions

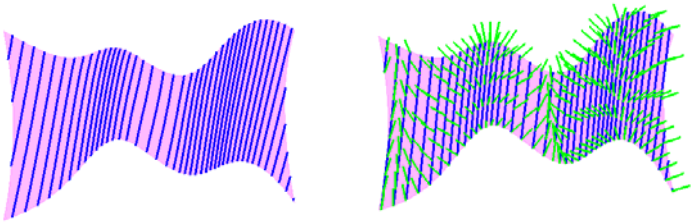

(c) Tool-paths on the surface (d) The cutter's postures at the CC points

Fig. 8. Cutting direction determination, tool-path and CL data generation.

Major radius R (mm)	*Minor radius r_f (mm)*						*Length (mm)*
12	0.5	1	1.5	2	2.5	3	110
10	0.5	1	1.5	2	2.5	3	100
8	0.5	1	1.5	2	2.5	3	90
6	0.5	1	1.5	2			80

Tab.1. The library of fillet-end cutters.

Firstly, the surface patch was sampled uniformly along u and v into 201×201 points. We then took the first cutter (12mm, 0.5mm) to evaluate the A-maps at all points. At point (76.2114, 45.2860, 15.6082), the A-map is "NULL". Therefore, this cutter is not accessible to this point and thus cannot be used to finish the entire surface. The next cutter in the list, i.e., cutter (12mm, 1mm), was then picked as the current cutter for A-map evaluation. This process was repeated until a feasible cutter, to which a non-empty A-map exists at every sampled point, was found. In this case, the cutter with (6mm, 0.5mm) was found to be the largest feasible cutter. The A-maps of cutter (6mm, 0.5mm) at all the sampled points were recorded.

The method presented in Section 3.2 was then applied to find the optimal cutting direction for an iso-planar path pattern by using cutter (6mm, 0.5mm). The range of [0, 360º] was sampled into 361 discrete angles with an increment of 1°. Fig. 8b shows the values of $(\sum_{i=1}^{n} \mathrm{PCR}_i / n)$, where n = 201×201, along the 361 angles. The direction with angle 275° from **X**-axis has the minimum $(\sum_{i=1}^{n} \mathrm{PCR}_i / n)$ and thus was taken as the optimal cutting direction.

Finally, the method introduced in Section 3.3 was used to generate the optimal tool-paths with CL data. The profile tolerance was specified as 0.1mm. The scallop height tolerance was set as 0.1 mm either. As a result, 45 paths were produced with 485 CC points in total. Fig. 8c illustrates the generated tool-paths on the surface. It can be seen that the CC points are much sparse compared to the sampled points. Finally, Fig. 8d shows the postures of the cutter at the CC points (only half of the CC points are shown here for a clearer view).

5. CONCLUSIONS

In this paper, a new integrated approach to process planning for 5-axis milling of sculptured surfaces is presented. The key to achieve the integration is the newly proposed accessibility map (A-map) of a cutter to a point on the part surface. The A-map is evaluated in respect of all the interference concerns, i.e., machine axis limits, local gouging, rear-gouging, and global-collision, while cutter feeding direction is not assumed. A method based on geometric analysis is introduced for obtaining the A-maps of a cylindrical cutter to the sampled points on a part surface. Subsequently, the A-maps can be used for process planning tasks such as cutter selection, cutting direction selection, and tool-path generation, in which various optimization objectives can be applied in a computationally efficient manner. One example is presented in this paper to demonstrate the effectiveness of this integrated approach. The authors believe that the concept of A-map provides a new dimension towards automated process planning for 5-axis finish machining of sculptured surfaces.

6. ACKNOWLEDGEMENTS

The work reported in this paper has been supported by ASTAR of Singapore under the project R265-000-176-305.

7. REFERENCES

[1] Choi, B. K., Park, J. W. and Jun, C. S., Cutter-location data optimization in 5-axis surface machining, *Computer-Aided Design*, Vol. 25, No. 6, 1993, pp 377-386.

[2] Ding, X., Mannan, M. A., Poo, A. N., Yang, D. C. H. and Han, Z., Adaptive iso-planar toolpath generation for machining of free-form surfaces, *Computer-Aided Design*, Vol. 35, 2003, pp 141-153.

[3] Jensen, C. G., Red, W. E. and Pi, J., Tool selection for five-axis curvature matched machining, *Computer-Aided Design*, Vol. 34, No. 3, 2002, pp 251-266.

[4] Lakkaraju, R. and Raman, S., Optimal NC path planning: is it really possible? *Computers & Industrial Engineering*, Vol. 19, 1990, pp 462-464.

[5] Lee, Y. S. and Chang, T. C., Automatic cutter selection for 5-axis sculptured surface machining, *International Journal of Production Research*, Vol. 34, No. 4, 1996, pp 977-998.

[6] Lee, Y. S., Non-isoparametric tool path planning by machining strip evaluation for 5-axis sculptured surface machining, *Computer-Aided Design*, Vol. 30, No. 7, 1998, pp 559-570.

[7] Li, L. L. and Zhang, Y. F., Cutter selection for 5-axis milling of sculptured surfaces based on accessibility analysis, to appear in *International Journal of Production Research*, 2005.

[8] Li, S. X. and Jerard, B., 5-axis machining of sculptured surfaces with a flat-end cutter, *Computer-Aided Design*, Vol. 26, No. 3, 1994, pp 165-178.

[9] Lin, R. S. and Koren, Y., Efficient tool-path planning for machining freeform surfaces, *ASME Journal of Engineering for Industry*, Vol. 118, 1996, pp 20-28.

[10] Morishige, K. and Takeuchi, Y., Tool path generation using C-space for 5-aixs control machining, *ASME Journal of Manufacturing Science and Engineering*, Vol. 121, 1999, pp 144-149.

[11] Pi, J., Red, W. E., and Jensen C. G., Grind-free tool path generation for five-axis surface machining, *Computer Integrated Manufacturing System*, Vol. 11, No. 4, 1998, pp 337-350.

[12] Vickers, G. W. and Quan, K. W., Ball-Mills versus end-Mills for curved surface machining, *ASME Journal of Engineering for Industry,* Vol. 111, 1989, pp 22-26.

[13] Xu, X. J., Bradley, C., Zhang, Y. F., Loh, H. T. and Wong, Y. S., Tool-path generation for five-axis machining of free-form surfaces based on accessibility analysis, *International Journal of Production Research*, Vol. 40, No. 14, 2002, pp. 3253-3274.